CHAPTER 7

CHAPTER 7

Geochronology

U-Pb radiometric study of zircon from representative samples of the study area was carried out using Sensitive High-Resolution Ion Microprobe (SHRIMP). U-Th-total Pb chemical dating of monazite was also carried out using Electron Microprobe (EPMA) on other representative samples of the study area.

7.1. Sample selection and description

Five samples from the high-grade rocks of the Central Gneissic Belt were selected for zircon U-Pb analyses (Fig. 7.1). Three samples from the southerly lying low-grade assemblages for monazite analyses were selected (Fig. 7.1). Metamorphic character and important field relation were given priority in selection of samples for geochronological analyses. The high-grade rocks from the Central Gneissic Belt represent deeper crustal section that witnessed amphibolite to granulite facies metamorphism, whereas the low-grade rocks from the supracrustal belts represents the shallow crustal section. Migmatitic and felsic gneiss samples have been analyzed to pinpoint the age of emplacement and metamorphism at mid-crustal conditions, whereas the granulites (charnockite and mafic granulite) proved helpful in determining the earlier tectonothermal events at deeper crustal conditions. Monazite analyses were done on samples from the low-grade supracrustal rocks of the Southern Supracrustal Belt to determine the time frame of the major tectonic (shearing) event. Detailed descriptions of the analyzed samples from the study area are presented in Table 7.1.

7.1.1 High-grade rocks of the Central Gneissic Belt

Sample RNG 120A (Charnockite gneiss)

This sample was collected from the central part of the Central Gneissic Belt along the E-W trending ridge south of the Rengali dam. The rock is mainly composed of orthopyroxene + clinopyroxene + K-feldspar + plagioclase + quartz ± garnet, where the gneissic foliations are marked by alternating orthopyroxene + garnet-bearing mafic layers and quartz + feldspar-rich leucocratic layers. Orthopyroxene occurs as small to medium-sized grain aggregates with quartz, plagioclase and K-feldspar to from the granulite assemblage and in places replaced by hornblende grains. Evidence of deformation is characterized by foliation-parallel stretching of quartz and feldspar grains. Zircon grains are present as major accessory minerals along with apatite and metamictized allanite.

Sample RNG 122 (Mafic granulite)

This sample of mafic granulite occurs as an enclave within charnockite gneiss at the central part of the Central Gneissic Belt near the Rengali dam site. The rock is distinctly foliated with few mm-thick alternate garnet-pyroxene rich layers and plagioclase-quartz rich layers. Coarse-grained garnet, clinopyroxene and plagioclase form the peak assemblage and the grains are extremely deformed. In some cases, hornblende forms along the margin of clinopyroxene. Zircon grains are few in number and are characteristically rounded in outline.

Sample RNG 129B (Migmatitic hornblende gneiss)

This is the main rock type of the Central Gneissic Belt. In outcrop-scale, this rock resembles the charnockite gneiss, but absence of orthopyroxene is discernable under microscopic study. In some quarry faces, charnockite gneiss occurs as patches and enclaves within this migmatitic hornblende gneiss. The sample is composed of hornblende + K-feldspar +

plagioclase + quartz + ilmenite + magnetite ± biotite ± garnet. Accessory phases like zircon and apatite are present.

Sample RNG 54D (Felsic gneiss)

This rock also constitutes the third category of the gneissic basement of the Central Gneissic Belt and shows a well-developed foliation defined by stretched quartz and feldspar. Effect of shearing and deformation are evident from mylonitic texture. The sample contains quartz + K-feldspar ± biotite ± plagioclase ± garnet. Accessory phases like zircon, ilmenite and apatite present.

7.1.2 Low-grade supracrustal belt of Rengali Province

Sample RNG 209 (Micaceous quartzite)

This sample was collected from a locality immediately adjacent to the footwall of South Riamol Splay. In this region, the prevalent greenschist-facies assemblage in muscovite schist changes to an amphibolite-grade assemblage of quartz-muscovite-sillimanite-fibrolite and is represented by the sample RNG 209. In this sample, breakdown of large muscovite flakes to alkali feldspar and fibrous aluminosilicate is observed, along with modal increase in magnetite-ilmenite lamellae. Monazite grains in Sample RNG 209 are concentrated along a thin zone containing magnetite, quartz, sillimanite and alkali feldspar.

Sample RNG 50D (Leucogranite)

The leucogranite occurs as a part of the basement gneiss for the quartzite-muscovite schist associations in the central part of the Rengali Province, close to its southern contact. It is mainly composed of quartz, alkali feldspar, plagioclase, biotite and some garnet

porphyroblasts. The rock is deformed in nature and cuspate grain boundaries of quartz and feldspar suggest that this rock may have evolved from a melt phase.

7.2 Analytical methods

Zircon grains for analyses were prepared by crushing and milling in Retsch disk mill followed by sieving, water separation and heavy liquid separation. To separate magnetic minerals from zircons, both Nd hand magnet and the Franz magnetic barrier separator at Presidency University, Kolkata were used. Extreme care was taken to avoid cross-contamination during sample preparation. Zircon grains were selected and handpicked for mounting at Hiroshima University. Epoxy mounts were prepared with zircon grains and the standard Duluth gabbroic anorthosite zircon (FC1) which has an age of 1099±0.6 Ma (Paces & Miller, 1993). The mounts were polished and gold coated for observation under the JEOL Scanning Electron Microscope (SEM) at the Hiroshima University. Backscatter electron (BSE) and Cathodoluminescence (CL) imaging were done for each zircon grain to study the internal morphology as well as locate zones for analysis. Analyses of zircon grains for U-Pb age dating were done at the SHRIMP-IIe facility at Earth and Planetary System Science Department of Hiroshima University in two analytical sessions. The external zircon standard (SL3) was used to measure U contents. Raw data were processed using the CONCH program (Nelson, 2006) while post-analysis data reduction was done based on the correction of the standard analyses. Each of the seven scans was checked and corrected, and those with anomalous counts were rejected. Processed data for all the samples are quoted in Table 7.2 with ±1σ uncertainty and plotted in a Wetherill diagram to obtain group ages. The ^{207}Pb-^{206}Pb group age calculations (with MSWD) were made using the program ISOPLOT 3.70 (Ludwig, 2008).

Monazite samples from micaceous quartzite (samples RNG 209) and leucogranite (Sample RNG 50D) were analyzed for U-Th-total Pb concentrations by JEOL JXA 8200 Superprobe at the Natural Science Center for Basic Research and Development (N-BARD), Hiroshima University. The operating conditions were 15 kV accelerating voltage, 200 nA beam current and 2-3 mm beam diameter. Standard materials are ThO_2 compound silicate glass and natural thorianite for Th, U_3O_8 compound silicate glass and natural uraninite for U and Pb-Te for Pb. The peak intensities of Th, U, and Pb were integrated for 60, 120, and 440 s, respectively. The detection limit of Pb at the 2s confidence level is of the order of 45 ppm, and the measurement errors of PbO are 55 ppm for 0.05wt.% level, and 66 ppm for 0.5 wt.% level, respectively. Basic principle of age dating using the U-Th-total Pb CHIME technique, developed by Suzuki & Adachi (1991) is used in case of these samples. However, the age calculation was carried out by employing an improved method of Cocherie and Albarede (2001) and plotted by ISOPLOT/EX 3.70 (Ludwig, 2008). The consistency of age data is cross-checked using a standard monazite of 1033 Ma (Hokada and Motoyoshi, 2006). Uncertainties in the individual analysis in the table and weighted mean ages are quoted at 95% confidence level. Results of all the monazite analyses are presented in Table 7.3.

7.3 Results

7.3.1 Zircon analysis of high-grade rocks of the Central Gneissic Belt

Sample RNG 120A (Charnockite gneiss)

Zircon grains in this sample are subhedral in outline with few grains of high aspect ratio. The size of the grains varies from 200-300 μm in length and 100-150 μm across. Almost all the grains exhibit core-mantle structure (Fig. 7.2) wherein the core region shows faint traces of oscillatory zoning with local high-U patches. A few grains contain relicts of xenocrystic cores. Large rounded inclusions of quartz are present in core regions of many grains. A

moderately thick (30-50 μm) high-U overgrowth zone is found in most of the grains. This overgrowth zone is featureless in most cases, but the presence of simple planar zoning is evident in some grains. The Th, U and Pb contents in the oscillatory zoned domains are fairly uniform (13-411 ppm, 53-121 ppm and 99-246 ppm respectively). The overgrowth domain is compositionally distinct to cores with high U (578-642 ppm), Pb (215-423 ppm) and highly variable Th (46-375 ppm) contents. The Th/U ratios from analyzed spots show minor variation for the oscillatory zoned zircon (0.25-0.65), whereas the overgrowth domain shows uniformly low values (0.08-0.16).

A total of 15 spots were analyzed from five grains. All but one spot data show reverse discordance (102-109%), even though U concentration is not very high in the analyzed spots. Nine spots from the oscillatory zoned zircon domain yield two statistical pools of data (95% conf.) of 2861±30 Ma (MSWD = 0.64; n= 3) and 2818±15 Ma (MSWD = 1.5; n= 6) (Fig 7.2). While the apparently unaltered oscillatory zoned domain shows a c. 2861 Ma date, the recrystallized oscillatory zoned domain, patches and overgrowths show a c. 2818 Ma date. Spots from the high-U overgrowth yield a third population of 2489±23 Ma (MSWD = 0.18; n=3) (Fig 7.2). This is possibly the age of a prominent thermal overprint. Two spot dates from the same domain define a somewhat younger pool date of 2451±8 Ma (1σ). Probability density plot shows two widely spaced peaks culminating at c. 2809 Ma and c. 2486 Ma respectively.

Sample RNG 122 (Mafic granulite)

Zircon grains in this sample are xenoblastic and mostly oval. The size of the grains varies from 150 to 200 μm across. All the grains show thick metamorphic overgrowths characterized by relatively bright CL domains surrounding darker cores. Zoning in the overgrowth domain is simple, with rare sector zoning (Fig. 7.3). Twelve spots from seven

zircon grains were analyzed in this sample. Multiple spots were chosen for each grain to determine the ages of different zircon domains. The U, Th and Pb contents vary even within a single grain. Th/U ratios vary in the range from 0.06-0.86. Spot data are nearly concordant to moderately discordant (86-104% concordance) and define six age groups (Fig. 7.3). The most dominant group yields a $^{207}Pb/^{206}Pb$ date of 2488±19 Ma (MSWD =1.5; 95% confidence, n= 4). Other groups give dates of 2844±7 Ma (MSWD = 0.47; 1σ; n=2) and 2351±34 Ma (MSWD = 1.12; 95% confidence; n=3). Two other spots yielded 2408±6 Ma (1σ) and 2351±34 Ma (95% confidence) dates. The older age domain of c. 2844 Ma is situated at the interior of the zircons and possibly reflects a crystallization age. However, moderate Th/U ratios (0.69-0.83) and faint zoning in this domain could also indicate a metamorphic origin. A limited number of data points and small geographical extent of the domain make any interpretation uncertain. The c. 2488 Ma (some spots with low Th/U ratios) is the most dominant tectonothermal event witnessed by this rock. Three groups of data younger than c. 2488 Ma are problematic. A few spot dates are nearly concordant (e.g. 6.4 in Table 7.2) and are positioned in the same grain adjacent to the c. 2488 Ma domain. As this sample does not contain much zircon, hence the result from the analytical data can be considered short of reaching any definite conclusion. A probability density plot for the $^{207}Pb/^{206}Pb$ spot data shows a strong peak at c. 2488 Ma followed by several smaller peaks of older and younger dates (Fig. 7.3).

Sample RNG 129B (Migmatitic hornblende gneiss)

Zircon grains are elongated prismatic in nature, having a high aspect ratio, although a few oval grains are also present. Most of the grains show high-CL oscillatory zoning with patches of high-U character (Fig 7.4). A few grains contain dark-CL cores. Seventeen spots were analyzed from fourteen grains. Except for spot 15.1 (Table 7.2), all others show uniform

Th/U ratios (0.51-0.72). Out of these, nine spots with near-concordant data yield a pooled age of 2828±9 Ma (95% conf., MSWD = 2.3; Fig 7.4). Two spots from the cores form a slightly older group with 2860±5 Ma (±1σ) date. Five spots from blurred oscillatory zoned domains are more discordant with ^{207}Pb-^{206}Pb dates younger than 2800 Ma. These spot dates possibly indicate differential Pb-loss from the oscillatory-zoned zircon due to partial destruction of zircon lattice (Mezger and Krogstad, 1997) although their U contents are not higher compared to the other spots. The spot 15.1 (Table 7.2) date was acquired from a planar-zoned exterior part of oscillatory-zoned zircon. The spot has a distinctly low Th/U ratio (0.07) and younger near-concordant spot date of 2471±4 Ma. The 2828±9 Ma age is therefore inferred to give the emplacement age of the protolith of the hornblende gneiss. All the zircon grains are variably disturbed by a later tectonothermal event. Probability density plot for 207Pb-206Pb ages shows a very strong peak at c. 2836 Ma (Fig 7.4).

Sample RNG 54D (Felsic gneiss)

Grains in this sample are mostly oval, 100-200 μm long and 50-150 μm across. Some grains have high aspect ratios. All grains have core-rim structure in CL and BSE imaging (Fig 7.5). Cores show moderate to high-CL faint oscillatory zoning truncated by a thick (30-50 μm) overgrowth. The latter domain has low-CL faint planar zoning or is unzoned. Some of the cores show a patchy dark interior surrounded by a thin bright-CL planar zoned domain. Fifteen grains were analyzed and twenty-two spots from these grains define three populations of data. Zircon cores of variable Th/U ratios (0.07-0.90) and yield a pooled age of 2776±24 Ma (95% conf., n=6; Fig 7.5). However, the age has very large scatter (MSWD = 42) presumably due to errors in individual spot analysis. The overgrowth domain yields a pooled age of 2508±14 Ma (95% conf., n=9; Fig 7.5), also with large scatter (MSWD = 30). Five spots from the overgrowth domain (Spots 1.1, 4.2, 7.1, 28.2 and 31.1) with a narrow range of

Th/U ratio (0.10-0.16; Table 7.2) yielded a third group with 2434±34 Ma (MSWD = 51). However, the spots show chemical characters (Th/U ratio) and CL or BSE response similar to other spots having c. 2508 Ma age. The probability density plot for $^{207}Pb/^{206}Pb$ ages shows three distinct peaks. It appears that the protolith of the felsic gneiss was emplaced during c. 2776 Ma and later metamorphosed during c. 2508 Ma (Fig. 7.5).

Sample RNG 50D (Leucogranite)

Zircon grains in this sample are subidioblastic to xenoblastic in nature and mostly oval. Elongated grains are 150-200 μm long and 50-100 μm across. Grains show faint traces of oscillatory zoning in the interior (Fig 7.6). The exterior part, on the other hand, shows blurred zonation and presence of thin high-U overgrowths (20-30 μm thick). Although Th, U and Pb contents vary considerably between successive zones, Th/U ratios from the analyzed spots vary within a narrow range (0.52-0.67). In comparison, Th/U ratio in the overgrowth domain is much lower (0.11). Seven grains were analyzed for a total of 10 spots. Spot data from the simple zoned zircon forms two distinct groups when plotted (Fig. 7.6). The majority of the data yield a $^{207}Pb/^{206}Pb$ pooled date of 2807±13 Ma (MSWD = 2.1; 95% confidence, n= 9). Only one spot could be measured from the overgrowth domain and it gives nearly concordant date of 2484±5 Ma (±1σ). The leucogranite was thus possibly emplaced at c. 2807 Ma and later metamorphosed at c. 2484 Ma. A probability density plot of $^{207}Pb/^{206}Pb$ spot data defines a very strong peak at c. 2805 Ma with a very weak peak at c. 2483 Ma (Fig. 7.6).

7.3.2 Monazite analysis of low-grade supracrustal rocks from the Rengali Province

Monazite grains in RNG 209 are irregular in shape with size varying from 50 mm to 100 mm at the long direction and are mostly associated with magnetite (containing exsolved ilmenite) grains (Fig. 7.7). Some of the grains occur as inclusions within magnetite that are associated

with quartz, K-feldspar, muscovite and sillimanite grains. Irregular patchy monazite also occurs at the margin of magnetite (Fig. 7.7). Thirty-seven spots from six analyzed monazite grains show compositional variation (Fig 7.7), but the calculated spot dates vary within a narrow range of ca. 507-554 Ma (Table 7.3). Unmixing of spot data defines two age peaks at 521 ± 3 Ma and 542 ± 5 Ma (Fig. 7.7). The former is more prominent (0.73 fraction, Fig 7.7) and this could indicate the age of thermal overprinting.

Monazite grains from the sample RNG 50D are much smaller with maximum size up to 50 mm x 30 mm. Grains are elongate, subhedral locally with corrugated outlines. BSE imaging shows almost homogeneous nature of the analyzed grains (Fig 7.8). Spot ages give a uniform single population age of 498 ±4Ma (n = 22, Fig 7.8). This is clearly identified in the probability density plot where the ca. 498 Ma peak appears very strong and can be considered as a tectonothermal event, related to the last phase of brittle deformations observed within the Rengali Province.

U-Pb zircon radiometric dating of the high-grade gneisses and granulites reveal that the main tectonothermal event took place in Rengali Province at around 2800 Ma followed 2500 Ma. All the high-grade rocks- charnockite, migmatitic hornblende gneiss, felsic gneiss and intrusive leucogranite, all shows peak ages 2809 Ma, 2836 Ma, 2776 Ma and 2805 Ma respectively. Hence, it can be confirmed that a major tectonothermal event related to these rocks took place around 2800 Ma. Again these high-grade rocks, as well as mafic granulite shows another strong peak around 2500 Ma (Charnockite- 2486 Ma, Mafic granulite- 2488 Ma, Felsic gneiss- 2508 Ma and leucogranite- 2483 Ma) related to a second phase of tectonothermal event. A comparative diagram of all the probability density plots is shown in Fig 7.9. Monazite grains from the supracrustal belt gives a peak age of around 500 Ma.

Monazite grains in the leucogranite of the Central Gneissic Belt shows a group age of 498 Ma, possibly related to the low-grade tectonothermal event.

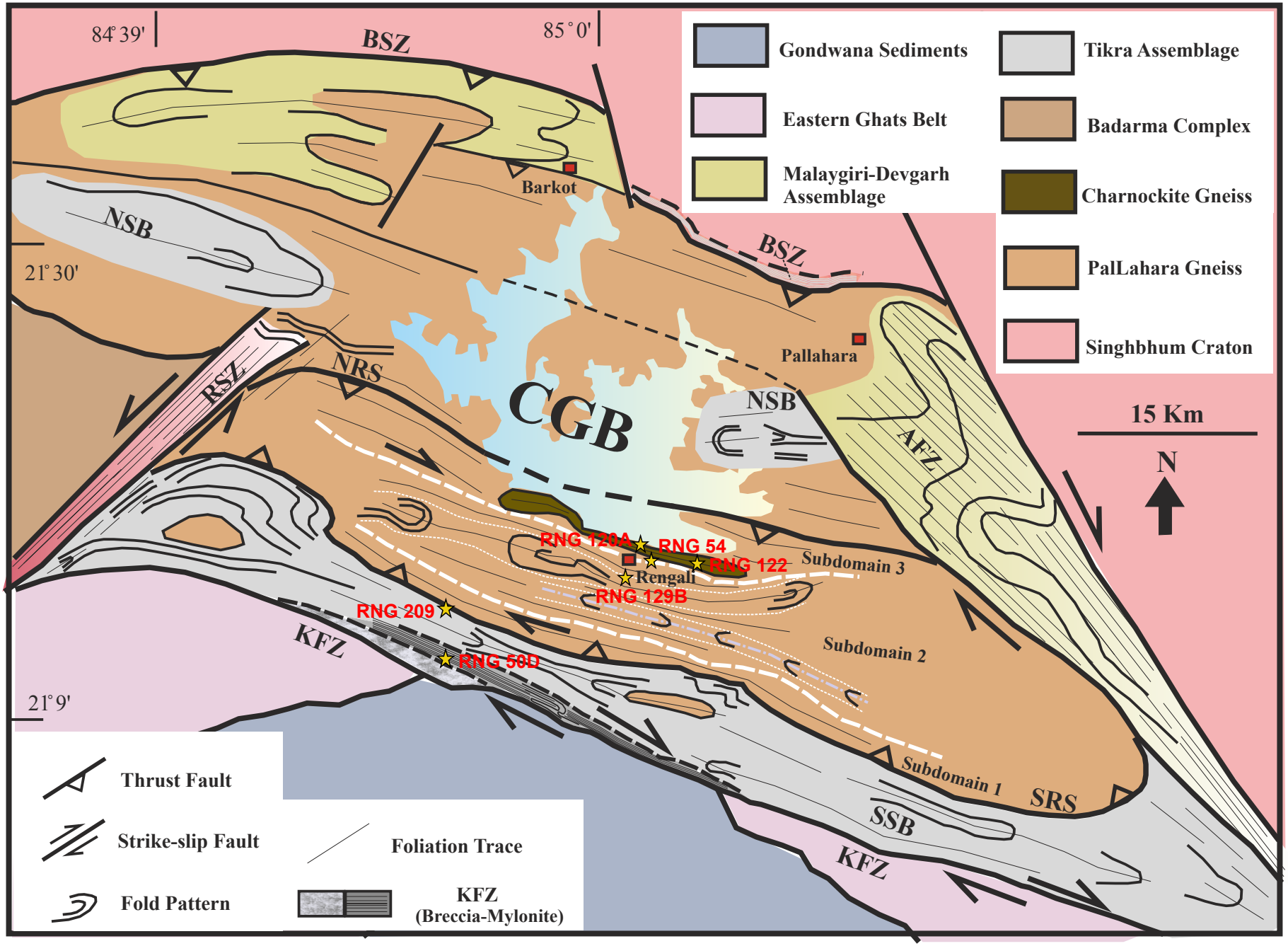

Fig. 7.1: Detailed map of central part of the Rengali Province, showing the locations of the analyzed geochronological samples.

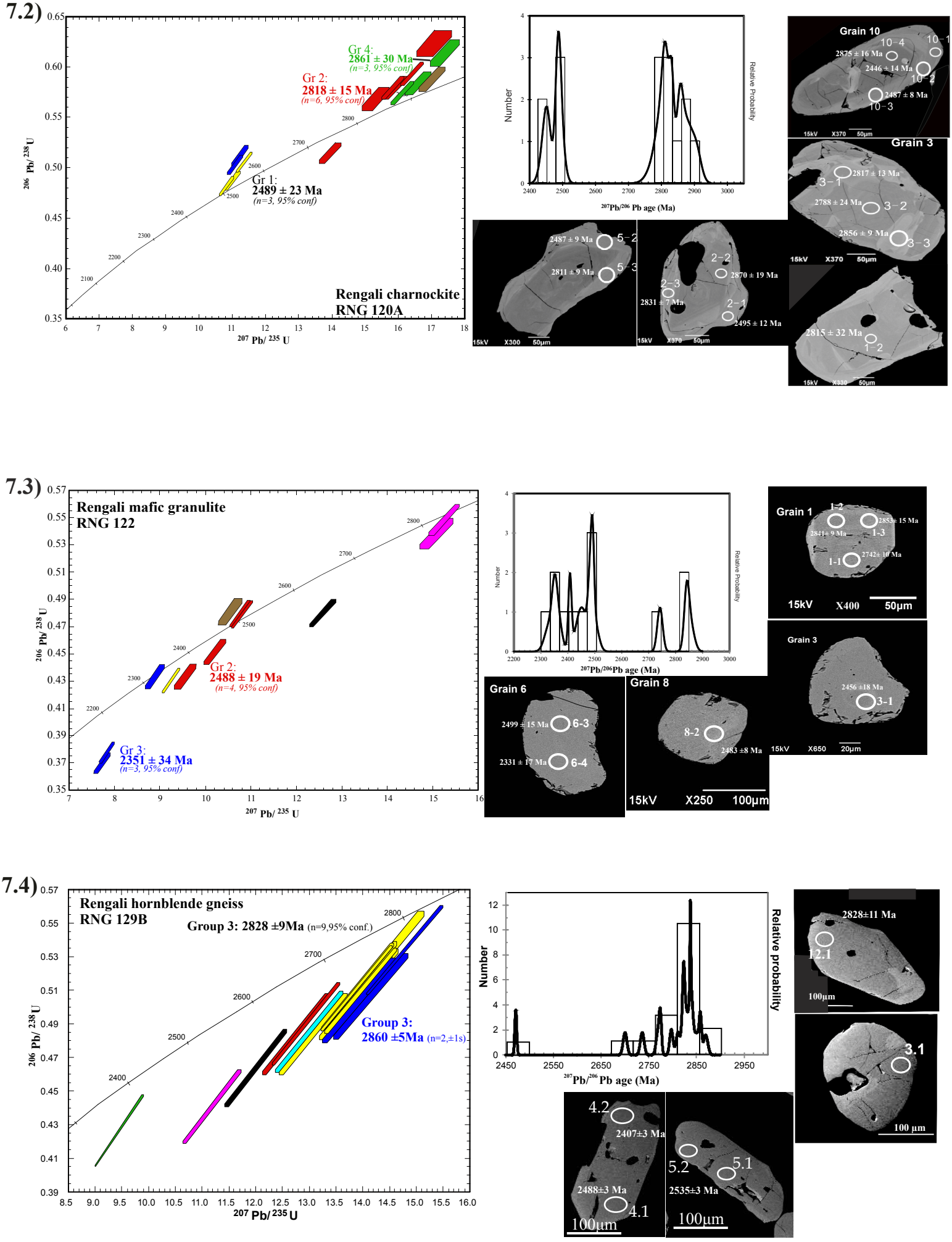

Weatherill plots of spot ages from samples of the Central Gneissic Belt Fig. (7.2) Charnockite (RNG 120A) (7.3) Mafic granulite (RNG 122) (7.4) Migmatitic hornblende gneiss (RNG 129B) showing group ages calculated using the program CONCH. Each plot also contains the probability density plot of $^{207}Pb/^{206}Pb$ ages. Backscatter electron (BSE) images of selected zircon grains from analyzed samples with spot positions and $^{207}Pb/^{206}Pb$ ages are also shown.

7.5)

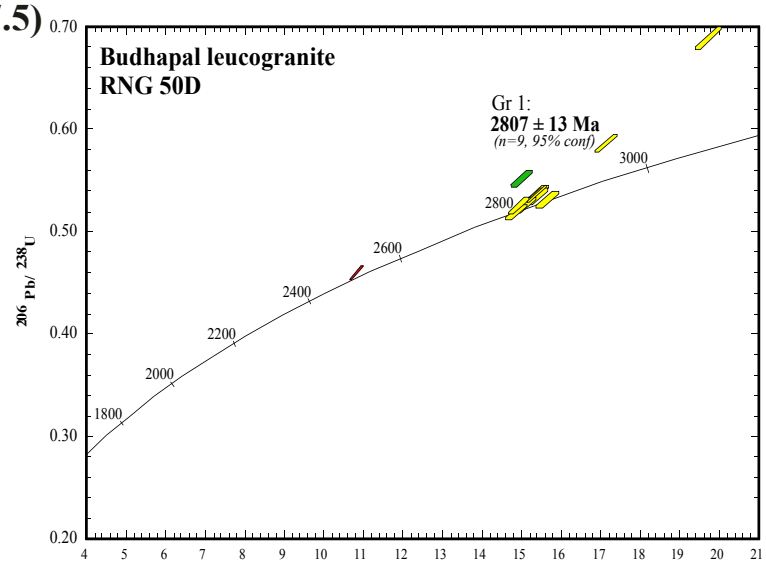

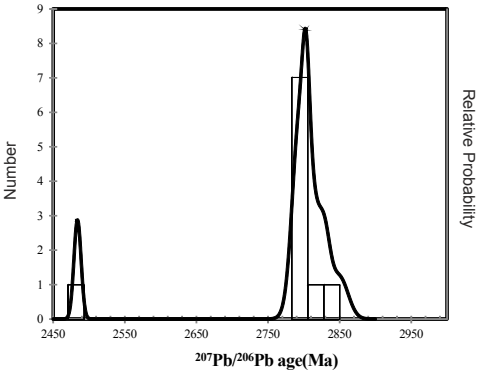

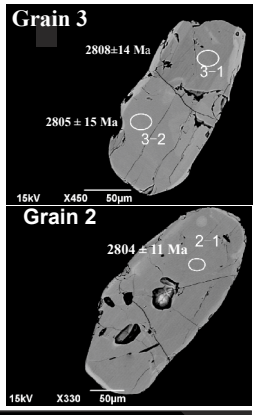

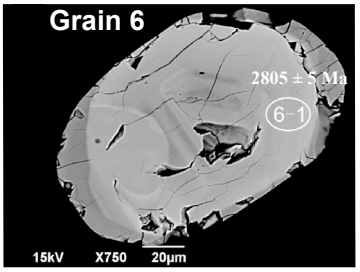

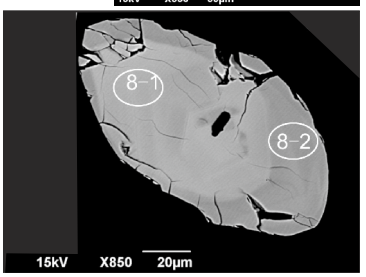

7.6)

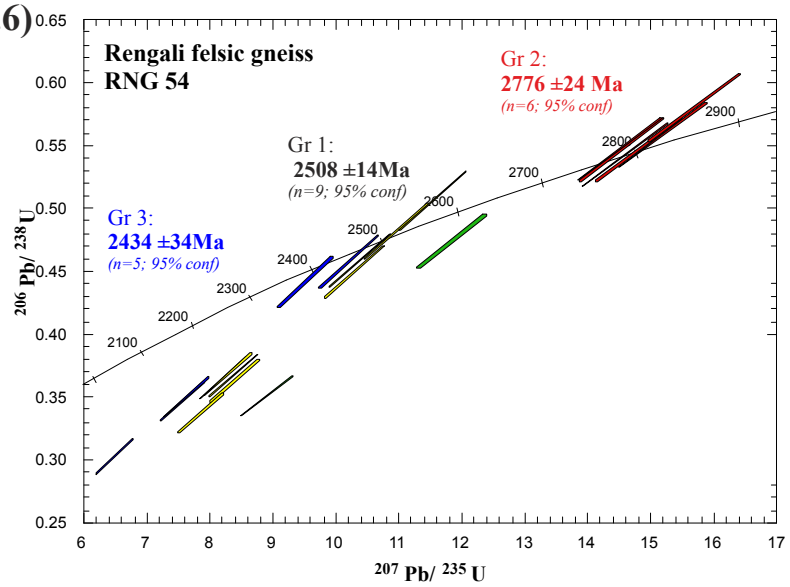

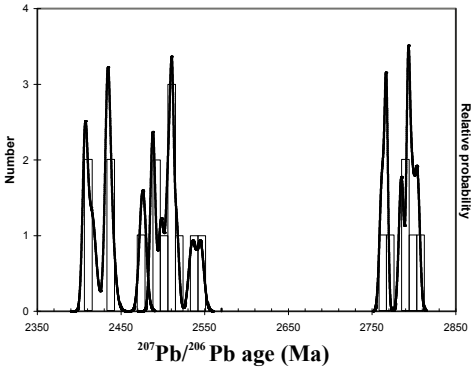

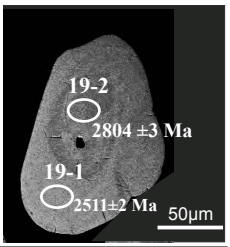

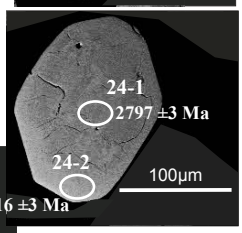

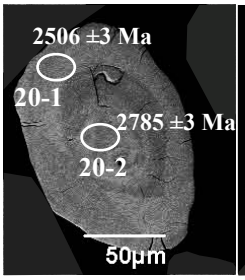

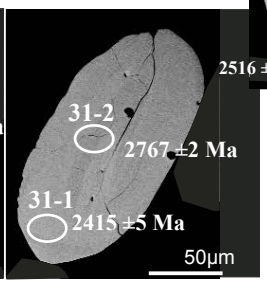

Weatherill plots of spot ages from samples of the Central Gneissic Belt Fig. (7.5) Felsic gneiss (RNG 54) (7.6) Leucogranite (RNG 50D) showing group ages calculated using the program CONCH. Each plot also contains the probability density plot of $^{207}Pb/^{206}Pb$ ages. Backscatter electron (BSE) images of selected zircon grains from analyzed samples with spot positions and $^{207}Pb/^{206}Pb$ ages are also shown.

7.7)

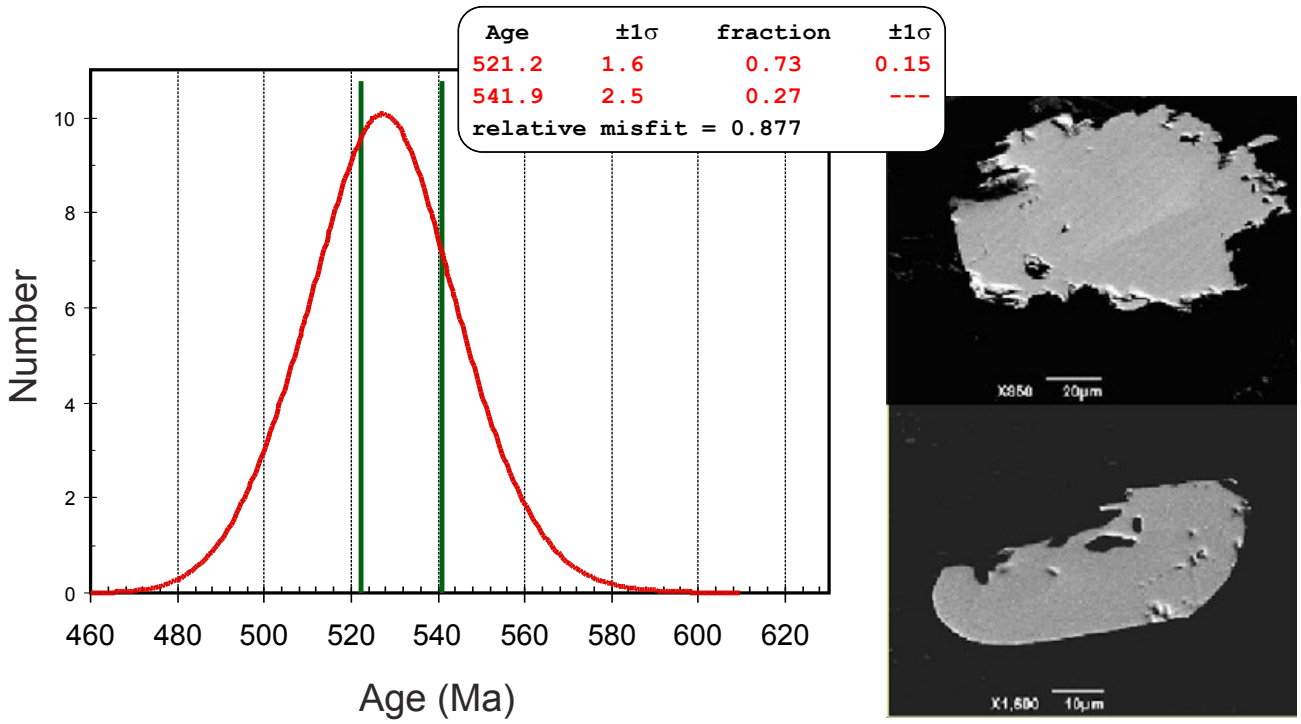

Fig.7.7: Unmixed spot ages showing two population for the sample RNG 209. On the right hand side, BSE images of analysed monazite grains.

7.8)

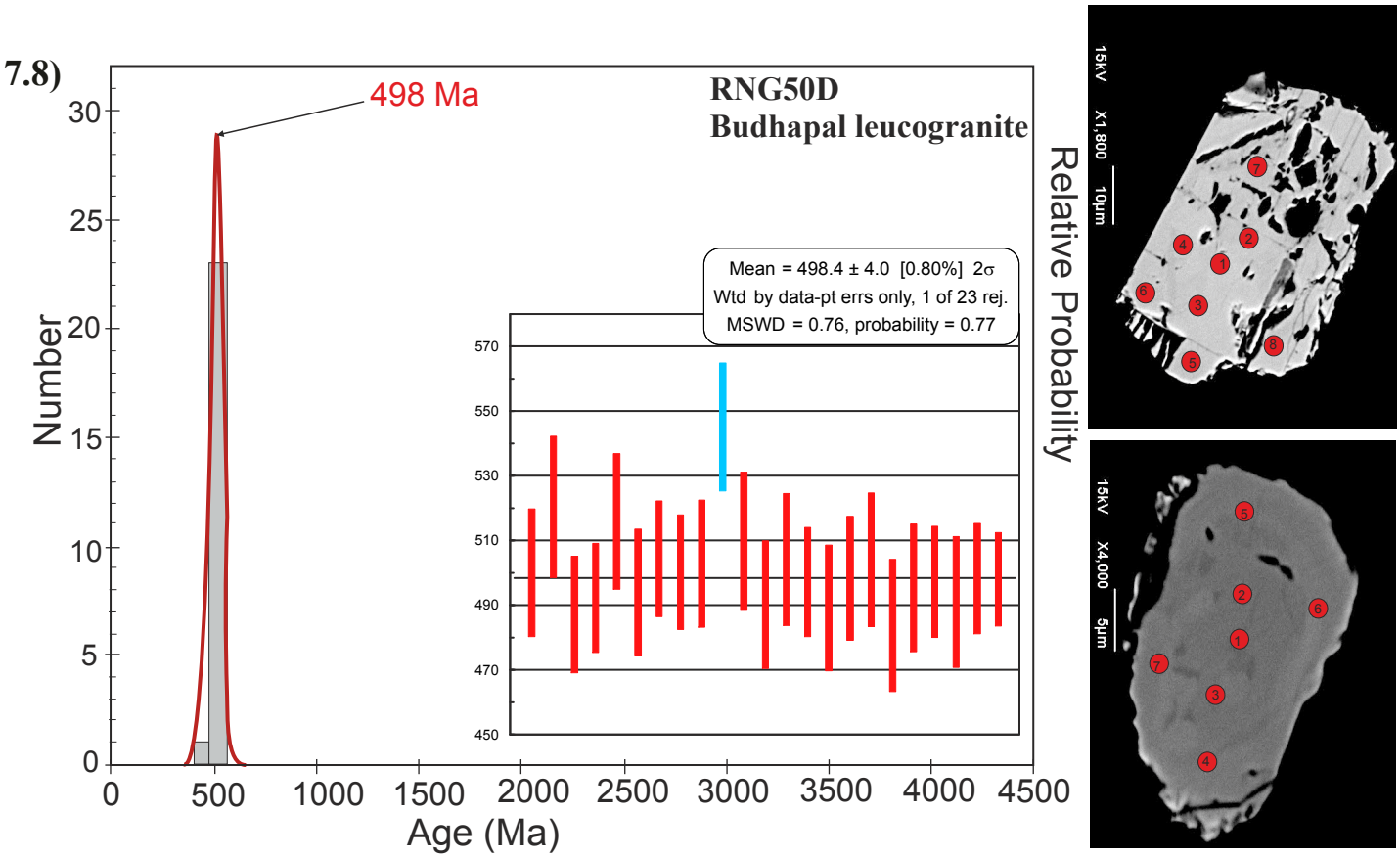

Fig.7.8: Probability density plot of monazite grains of the leucogranite (RNG 50D). Inset- shows weighted average of mean ages from RNG 50D.On the right hand side, BSE images of analyzed monazite grains with spot positions.

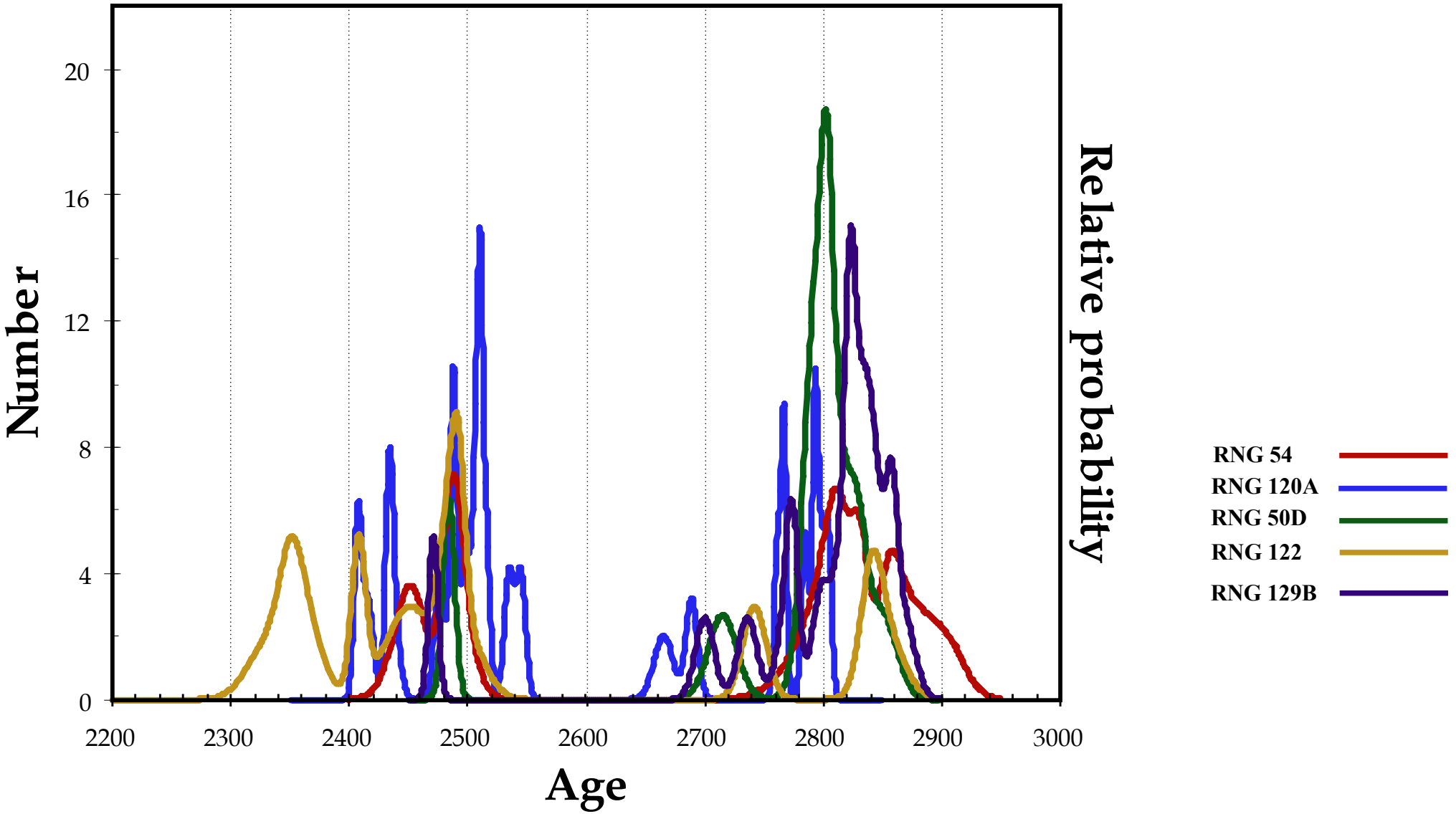

Fig. 7.9: Probability density plot the calculated ages from U-Pb zircon analysis of of all the high-grade samples of the Central Gneissic Belt.

Table 7.1: Summary of the samples collected form Central Gneissic Belt and supracrustal units for geochronological study

Sample no.	Location	Dating method	Rock type	Mineral assemblage	Deformational history and metamorphism	Age Summary
RNG 120A	21°16′31.70″N 85°1′49.89″E	U-Pb Zircon dating using SHRIMP	Charnockite	Kfs+Qrtz+Opx±Cpx+Hbl+ Ilm+Zrn	S2 gneissic banding present. Opx grains show retrograde metamorphism texture. In this part of CGB, charnockite had undergone a much lower garde of metamorphism, at the mid-crustal level.Opx grains show retrograde metamorphism texture. In this part of CGB, charnockite had undergone a much lower garde of metamorphism, at the mid-crustal level.	2861±30 Ma : emplacement age of the Charnockite; 2818±15 Ma : metamorphic age; 2489±23 Ma : second phase of metamorphic overprinting
RNG 129B	21°15′14.34″N 85°1′6.6″E	U-Pb Zircon dating using SHRIMP	Migmatitic hornblende gneiss	Hbl+Pl+Qtz+Kfs±Ap+Ilm+Zr n	Gneissic banding is shown by deformed Hbl grains. Suffers an amphibolite grade metamorphism.	2860 ±5 Ma: Protolith age; 2828±9 Ma : magmatic emplacement age; 2471±4 Ma: the second metamorphic event
RNG 54	21°16′9.72″N 85°2′15.18″E	U-Pb Zircon dating using SHRIMP	Felsic gneiss	Qrtz+Kfs +Bt+Zrn+Plag +Gt	The rock shows S2 mylonitic fabric with Kfs porphyroclasts surrounded by finer grained tails.	2776±24 Ma: magmatic emplacement age; 2508± 14 Ma: the second metamorphic event
RNG 122	21°15′33.32″N 85°4′4.83″E	U-Pb Zircon dating using SHRIMP	Mafic granulite	Grt+Cpx+Pl+Qtz+Hbl+Opx+Il m+Zrn	Show effect of strong shear along S2. Gneissic banding is present with deformed Grt + Cpx forming mafic layers. Occur as enclaves within the charnockite. These mafic granulites suffered an earlier high pressure metamorphism, followed by cooling phase.	2844±7 Ma : Crystallization age or metamorphism age (due to presence of faint zoning , moderate Th/U) 2488±19 Ma: the second phase of metamorphism and reworking
RNG 50D	21°12′1.12″N 84°52′49.31″E	U-Pb Zircon dating using SHRIMP	Intrusive leucogranite	Qtz+Kfs+Pl+Grt+Mus+Zrn+M nz	Abundant muscovite showing a weak foliation, post-kinematic Grt present. Evidence of melt crystallization.	2807 ±13 Ma: emplacement age; 2484±5 Ma: the second metamorphic event
RNG 209	21°14'19.42"N 84°53'3.35"E	U-Pb-Th monazite chemical age dating using EPMA	Mica schist-fibrolite	Qrtz+Mus+Kfs+Sil+Fibrolite+ Mag+Ilm	At the footwall of SRS, prevalent greenschist grade changes to amphibolite grade, evident from appearance of sillimanite grains.	521±3 Ma: A low grade tectono-thermal overprinting (thrusting along the southern margin of RP)
RNG 50D	21°12′1.12″N 84°52′49.31″E	U-Pb-Th monazite chemical age dating using EPMA	Intrusive, sheared leucogranite	Qtz+Kfs+Pl+Grt+ Mus+Zrn+Mnz	Abundant muscovite showing a weak foliation, post-kinematic Grt present. Evidence of melt crystallization.	498±4 Ma: timing of dextral sheraing along KFZ.

Table 7.2: Ion microprobe analytical results for zircons from samples

Grain	U (ppm)	Th (ppm)	Pb (ppm)	Th/U (ppm)	$^{207}Pb/^{206}Pb$	±1σ	$^{208}Pb/^{206}Pb$	±1σ	$^{206}Pb/^{238}U$	±1σ	$^{207}Pb/^{235}U$	±1σ	% concordance	$^{207}Pb/^{206}Pb$ Age	±1σ
RNG 120A															
1.1	312	118	207	0.378	0.20987	0.00189	0.10363	0.0023	0.5879	0.012	17.011	0.396	103	2905	15
1.2	139	87	103	0.626	0.19867	0.0039	0.18309	0.00745	0.6233	0.0133	17.076	0.526	111	2815	32
2.1	463	75	234	0.162	0.16381	0.00112	0.04436	0.00149	0.4869	0.0096	10.997	0.239	102	2495	12
2.2	138	81	100	0.587	0.20545	0.00237	0.15592	0.00345	0.6142	0.0127	17.399	0.433	108	2870	19
2.3	618	193	408	0.312	0.2006	0.0009	0.0886	0.00076	0.5933	0.0117	16.41	0.34	106	2831	7
3.1	207	108	139	0.522	0.19894	0.00157	0.1488	0.00157	0.5796	0.0117	15.899	0.359	105	2817	13
3.2	144	88	97	0.611	0.19544	0.00282	0.17642	0.005	0.5684	0.0117	15.318	0.407	104	2788	24
3.3	627	375	426	0.598	0.20364	0.00109	0.17242	0.00157	0.5744	0.0113	16.127	0.34	102	2856	9
5.1	581	53	298	0.091	0.15983	0.001	0.02424	0.00108	0.5031	0.0099	11.087	0.238	107	2454	11
5.2	645	59	318	0.091	0.16301	0.00086	0.02467	0.00055	0.4818	0.0095	10.83	0.228	102	2487	9
5.3	628	46	382	0.073	0.19812	0.0011	0.02134	0.00174	0.5794	0.0114	15.828	0.335	105	2811	9
5.4	212	54	120	0.255	0.19662	0.00181	0.07823	0.00147	0.5148	0.0104	13.955	0.325	96	2798	15
10.2	413	102	223	0.247	0.15913	0.0013	0.06926	0.00193	0.5122	0.0102	11.239	0.252	109	2446	14
10.3	612	97	323	0.158	0.16303	0.00079	0.04729	0.00068	0.5054	0.0099	11.362	0.236	106	2487	8
10.4	132	74	90	0.561	0.20611	0.00205	0.15777	0.00384	0.5838	0.0116	16.592	0.387	103	2875	16
RNG 50D															
1.1	434	291	290	0.671	0.19563	0.0012	0.20305	0.00126	0.5536	0.0086	14.932	0.26	102	2790	10
2.1	160	91	102	0.569	0.19731	0.00134	0.16124	0.00154	0.5464	0.0085	14.864	0.263	100	2804	11
2.2	148	87	98	0.588	0.20289	0.00146	0.16358	0.00215	0.5596	0.0087	15.653	0.281	101	2850	12
3.1	114	65	75	0.570	0.19784	0.00172	0.15133	0.00277	0.5632	0.0088	15.363	0.29	103	2808	14
3.2	109	58	71	0.532	0.19738	0.00175	0.14365	0.0028	0.5658	0.0089	15.399	0.292	103	2805	15
4.1	138	92	94	0.667	0.18689	0.00141	0.1744	0.00196	0.5821	0.0091	14.999	0.272	109	2715	12
4.2	822	91	407	0.111	0.16268	0.00051	0.03202	0.00026	0.4823	0.0073	10.818	0.172	102	2484	5
4.3	106	56	68	0.528	0.19755	0.00154	0.14404	0.00263	0.5539	0.0087	15.088	0.277	101	2806	13
6.1	1182	634	776	0.536	0.19718	0.00059	0.15105	0.0005	0.5656	0.0087	15.378	0.245	103	2803	5
7.1	987	701	852	0.710	0.19571	0.0009	0.17539	0.00098	0.7312	0.0113	19.732	0.33	127	2791	8
8.2	802	428	578	0.534	0.20037	0.00097	0.14946	0.00083	0.62	0.0096	17.127	0.288	110	2829	8
RNG 122															
1.1	136	113	81	0.831	0.18995	0.00114	0.222	0.00209	0.48	0.0101	12.571	0.283	92	2742	10
1.2	190	132	126	0.695	0.20183	0.00109	0.19173	0.00141	0.5484	0.0115	15.26	0.339	99	2841	9
1.3	274	228	183	0.832	0.20334	0.00192	0.23906	0.00403	0.5382	0.0112	15.09	0.362	97	2853	15
2.1	152	131	68	0.862	0.15155	0.00121	0.24701	0.00193	0.3697	0.0077	7.725	0.18	86	2364	14
3.1	84	25	40	0.298	0.16001	0.00174	0.0834	0.00259	0.4332	0.0092	9.557	0.239	94	2456	18
5.1	196	12	75	0.061	0.15049	0.00084	0.01572	0.00115	0.3774	0.0079	7.83	0.174	88	2351	10

	5.2	618	67	272	0.108	0.15554	0.00056	0.03072	0.00034	0.4306	0.0089	9.235	0.198	96	2408	6
	6.3	87	51	46	0.586	0.16416	0.00145	0.16464	0.00254	0.4513	0.0094	10.215	0.241	96	2499	15
	6.4	74	44	37	0.595	0.14874	0.00144	0.16893	0.0027	0.4333	0.009	8.885	0.214	100	2331	17
	7.1	492	37	241	0.075	0.16347	0.00057	0.02236	0.00029	0.4791	0.0099	10.798	0.231	101	2492	6
	8.1	67	46	38	0.687	0.15892	0.00185	0.18746	0.00375	0.4809	0.01	10.537	0.264	104	2444	20
	8.0	315	182	173	0.578	0.16263	0.00074	0.16458	0.00085	0.4798	0.0099	10.76	0.233	102	2483	8
RNG 54																
	1.1	682	70	241	0.103	0.15824	0.00048	0.02749	0.00028	0.3468	0.0161	7.567	0.354	79	2437	5
	2.1	790	58	452	0.073	0.19227	0.00036	0.02119	0.00021	0.5472	0.0253	14.505	0.675	102	2762	3
	2.2	756	160	366	0.212	0.1641	0.00034	0.06033	0.00026	0.459	0.0212	10.385	0.484	97	2498	3
	3.1	1274	93	473	0.073	0.16308	0.00029	0.01996	0.0002	0.3654	0.0169	8.217	0.382	81	2488	3
	4.1	1593	898	621	0.564	0.16312	0.00027	0.06415	0.00033	0.368	0.017	8.276	0.385	81	2488	3
	4.2	1318	201	409	0.153	0.15546	0.00032	0.03636	0.00029	0.3025	0.014	6.484	0.302	71	2407	3
	5.1	813	228	321	0.280	0.1677	0.00038	0.09373	0.00045	0.3627	0.0168	8.387	0.391	79	2535	4
	6.1	1653	232	628	0.140	0.16515	0.00027	0.03848	0.00029	0.3675	0.017	8.368	0.389	80	2509	3
	7.1	1439	215	521	0.149	0.158	0.0003	0.04245	0.0003	0.3497	0.0162	7.619	0.355	79	2434	3
	8.1	1063	528	401	0.497	0.16877	0.00036	0.1311	0.00048	0.3374	0.0156	7.85	0.366	74	2545	4
	9.1	558	100	209	0.179	0.18396	0.00051	0.05216	0.00057	0.351	0.0163	8.904	0.416	72	2689	5
	19.1	2077	177	1077	0.085	0.16533	0.00024	0.02516	0.00011	0.5061	0.0234	11.537	0.536	105	2511	2
	19.2	1061	955	748	0.900	0.19724	0.00035	0.26747	0.00042	0.5584	0.0258	15.186	0.707	102	2804	3
	20.1	1304	198	654	0.152	0.16489	0.00031	0.0436	0.00018	0.4821	0.0223	10.96	0.51	101	2506	3
	20.2	1637	1000	1033	0.611	0.195	0.0003	0.15283	0.00029	0.5429	0.0251	14.596	0.679	100	2785	3
	23.1	88	56	49	0.636	0.18134	0.00085	0.1764	0.00133	0.4737	0.0219	11.844	0.558	94	2665	8
	24.1	1148	309	687	0.269	0.19644	0.00034	0.07493	0.00019	0.5467	0.0253	14.808	0.689	101	2797	3
	24.2	1168	192	546	0.164	0.16584	0.0003	0.04208	0.00015	0.4498	0.0208	10.286	0.479	95	2516	3
	28.1	1657	168	1016	0.101	0.19603	0.00026	0.03156	0.00011	0.5804	0.0269	15.686	0.729	106	2793	2
	28.2	1060	169	505	0.159	0.16196	0.00036	0.04938	0.00021	0.4571	0.0212	10.209	0.476	98	2476	4
	31.1	437	48	197	0.110	0.15619	0.00046	0.03293	0.00034	0.4416	0.0204	9.511	0.445	98	2415	5
	31.2	1130	454	689	0.402	0.19291	0.00029	0.10228	0.00028	0.5466	0.0253	14.538	0.676	102	2767	2
RNG 129B																
	2.2	104	54	53	0.519	0.18523	0.00089	0.14435	0.00134	0.4439	0.0262	11.336	0.679	88	2700	8
	3.1	125	64	74	0.512	0.19933	0.00074	0.13374	0.00094	0.5126	0.0303	14.087	0.84	95	2821	6
	4.1	188	126	120	0.670	0.20393	0.0006	0.1773	0.00089	0.5329	0.0315	14.985	0.891	96	2858	5
	4.2	174	120	102	0.690	0.19374	0.00062	0.18662	0.00092	0.491	0.029	13.117	0.781	93	2774	5
	5.1	141	81	80	0.574	0.19816	0.00092	0.15468	0.00131	0.4854	0.0287	13.262	0.794	91	2811	8
	5.2	156	91	94	0.583	0.20006	0.00088	0.15759	0.00131	0.5134	0.0303	14.162	0.847	94	2827	7
	6.1	98	71	61	0.724	0.20168	0.0012	0.20349	0.002	0.5091	0.0301	14.158	0.852	93	2840	10
	7.1	123	74	73	0.602	0.20527	0.00111	0.16321	0.0018	0.5068	0.03	14.344	0.861	92	2869	9
	8.1	119	88	70	0.739	0.19315	0.00099	0.2048	0.00155	0.4854	0.0287	12.926	0.775	92	2769	8
	9.1	152	89	91	0.586	0.20143	0.00083	0.15817	0.00109	0.5099	0.0301	14.161	0.846	94	2838	7

10.1	104	63	62	0.606	0.20135	0.00112	0.15799	0.0017	0.5061	0.0299	14.052	0.845	93	2837	9
11.1	137	80	78	0.584	0.19645	0.00084	0.16523	0.00101	0.4866	0.0288	13.181	0.788	91	2797	7
11.2	157	92	93	0.586	0.20301	0.00108	0.16594	0.00191	0.5044	0.0298	14.119	0.847	92	2851	9
12.1	115	63	70	0.548	0.20026	0.00134	0.15789	0.00246	0.53	0.0313	14.634	0.883	97	2828	11
13.1	340	208	205	0.612	0.1996	0.00055	0.16755	0.00072	0.5115	0.0302	14.077	0.837	94	2823	4
14.1	181	112	99	0.619	0.18934	0.00092	0.16711	0.00158	0.4659	0.0275	12.164	0.728	90	2736	8
15.1	875	63	383	0.072	0.16148	0.00039	0.01995	0.00022	0.4302	0.0254	9.578	0.569	93	2471	4

Table 7.3 Monazite electron microprobe data with calculated spot ages from Fibrolite Schist and Leucogranite sample

Data Point	Al_2O_3	SiO_2	P_2O_5	CaO	Y_2O_3	La_2O_3	Ce_2O_3	Pr_2O_3	Nd_2O_3	Sm_2O_3	Gd_2O_3	Dy_2O_3	PbO	ThO_2	UO_2	SO3	Total	**Age (Ma)**	**Age err**
Sample RNG 209																			
Grain 5																			
Mnz5-1	0	0.652	29.767	2.608	2.657	10.64	31.766	1.771	4.834	2.074	0.587	0.55	0.309	11.858	0.611	0.247	100.93	517	15
Mnz5-2	0	0.841	29.471	3.319	1.538	10.47	30.986	1.685	4.337	1.949	0.516	0.45	0.373	15.583	0.281	0.38	102.18	526	12
Mnz5-3	0	0.336	29.811	3.003	3.002	10.093	30.831	1.666	4.574	2.024	0.58	0.564	0.373	10.864	1.762	0.259	100.53	521	13
Mnz5-4	0	0.667	30.579	2.65	2.678	10.373	31.415	1.789	4.754	2.191	0.542	0.583	0.311	12.138	0.596	0.225	100.7	513	14
Mnz5-5	0	0.603	29.364	2.561	2.642	10.445	31.646	1.738	4.709	2.198	0.587	0.506	0.296	11.5	0.607	0.248	99.65	510	15
Mnz5-6	0	0.673	29.764	2.733	2.828	10.261	31.371	1.691	4.782	2.113	0.563	0.637	0.317	12.226	0.662	0.245	100.87	511	14
Grain 6																			
Mnz6-1	0	0.094	31.036	3.236	2.937	10.279	30.397	1.712	4.523	2.045	0.528	0.576	0.429	10.675	2.383	0.249	101.1	539	12
Mnz6-2	0	0.395	30.295	3.285	1.575	10.153	30.699	1.743	4.574	2.059	0.535	0.42	0.397	12.034	1.577	0.221	99.96	536	13
Mnz6-3	0	0.229	30.34	4.087	1.882	9.477	28.065	1.516	3.828	1.753	0.412	0.368	0.562	14.453	3.179	0.175	100.33	526	9
Mnz6-4	0	0.111	31.157	3.626	2.792	9.848	29.849	1.602	4.339	1.802	0.42	0.549	0.472	11.889	2.681	0.207	101.34	531	11
Grain 7																			
Mnz7-1	0	0.109	30.852	3.173	2.863	10.108	30.872	1.715	4.521	1.896	0.507	0.604	0.381	10.922	1.811	0.236	100.57	525	13
Mnz7-2	0	0.089	30.522	3.182	3.146	10.027	30.203	1.718	4.396	1.962	0.51	0.574	0.405	10.298	2.287	0.271	99.59	527	15
Mnz7-3	0	0.645	29.753	2.597	2.563	10.419	31.575	1.738	4.905	2.1	0.46	0.494	0.308	12.277	0.39	0.175	100.4	529	12
Mnz7-4	0	0.692	29.788	2.573	2.439	10.371	31.678	1.851	4.964	2.028	0.538	0.526	0.301	12.536	0.354	0.158	100.8	510	14
Mnz7-5	0	0.67	29.733	2.722	2.523	10.312	30.977	1.765	4.64	2.093	0.538	0.549	0.316	12.43	0.627	0.242	100.14	507	14
Mnz7-6	0	0.623	30.237	2.654	1.581	10.118	32.532	1.892	5.6	2.266	0.631	0.456	0.322	11.922	0.569	0.265	101.67	541	15
Mnz7-7	0	0.639	29.766	2.627	2.814	10.245	31.392	1.795	5.036	2.056	0.526	0.589	0.303	12.237	0.417	0.204	100.65	516	15
Grain 8																			
Mnz8-1	0	0.144	31.428	4.314	1.987	9.25	27.613	1.513	3.959	1.759	0.498	0.415	0.643	13.822	4.42	0.101	101.86	530	9
Mnz8-2	0	0.137	30.868	3.587	2.645	9.738	29.517	1.588	4.297	1.892	0.461	0.461	0.471	12.136	2.708	0.209	100.72	522	11
Mnz8-3	0	0.112	31.472	3.521	2.651	10.23	30.346	1.653	4.382	1.859	0.477	0.514	0.442	11.789	2.469	0.227	102.14	518	11
Grain 12																			
Mnz12-1	0	0.681	29.807	2.839	1.464	10.197	31.839	1.791	4.944	2.095	0.592	0.35	0.342	13.444	0.349	0.226	100.96	544	14
Mnz12-2	0	1.594	27.811	3.806	1.583	8.627	26.639	1.479	3.942	1.641	0.485	0.46	0.53	21.223	0.316	0.236	100.37	554	10
Mnz12-3	0	0.271	30.725	2.22	1.342	12.114	35.332	1.933	4.963	2.373	0.516	0.316	0.23	8.484	0.359	0.472	101.65	549	20
Mnz12-4	0	0.118	30.595	3.435	2.542	9.878	29.85	1.605	4.363	1.901	0.389	0.535	0.463	11.661	2.515	0.189	100.04	541	11
Mnz12-5	0	0.723	30.033	2.669	2.487	10.265	31.369	1.779	4.766	2.081	0.527	0.509	0.317	12.895	0.367	0.25	100.98	521	14
Mnz12-6	0	0.124	31.013	3.195	3.017	9.937	30.854	1.68	4.633	2	0.532	0.623	0.394	10.964	1.929	0.193	101.14	530	13
Mnz12-7	0	0.68	30.248	2.605	2.5	10.435	31.962	1.781	4.87	2.124	0.53	0.521	0.3	12.512	0.354	0.169	101.6	509	14
Mnz12-8	0	0.596	30.174	2.592	2.821	10.263	31.733	1.807	4.932	2.266	0.524	0.564	0.294	11.807	0.46	0.203	101.03	512	15
Grain 13																			
Mnz13-1	0	0.622	30.122	2.608	2.721	10.404	31.679	1.723	4.786	2.135	0.555	0.563	0.31	11.833	0.619	0.23	100.91	518	15
Mnz13-2	0	0.677	29.945	2.751	2.575	9.96	30.959	1.795	4.976	2.102	0.505	0.549	0.322	17.629	0.617	0.181	100.51	512	14
Mnz13-3	0	0.309	30.511	4.598	1.948	8.826	26.964	1.496	3.892	1.628	0.35	0.459	0.573	12.592	2.164	0.244	101.59	540	9
Mnz13-4	0	0.361	30.763	2.37	1.113	12.222	35.687	1.83	4.817	2.234	0.445	0.229	0.236	8.889	0.372	0.58	102.15	539	19
Mnz13-5	0	0.508	30.5	2.171	2.954	10.172	31.057	1.733	4.82	2.063	0.596	0.546	0.263	11.997	0.369	0.248	101.45	546	18

Mnz13-6	0	0.573	30.121	2.669	1.456	10.787	34.385	1.927	5.447	2.484	0.589	0.388	0.31	11.877	0.46	0.221	100.29	532	15
Mnz13-7	0	0.598	30.188	2.609	3.098	10.204	31.122	1.79	4.932	2.105	0.589	0.654	0.307	9.935	0.572	0.212	100.86	519	15
Mnz13-8	0	0.62	29.813	2.57	2.684	10.333	31.364	1.807	4.845	2.229	0.559	0.563	0.307	11.692	0.617	0.247	100.25	520	15
Mnz13-9	0	0.642	30.567	2.561	2.576	10.429	31.74	1.733	4.87	2.055	0.638	0.525	0.308	11.704	0.629	0.243	101.22	519	15
Sample RNG 50D																			
Grain 1																			
Mnz1-1	0	0.2337	31.5229	1.2337	2.7266	13.4991	28.2848	2.8324	8.4554	4.9471	1.6845	0.9283	0.2185	4.3656	1.6693	0	102.6018	500	20
Mnz1-2	0	0.539	29.9549	1.6105	2.2906	14.0459	28.7517	2.8941	7.9668	4.8218	1.2959	0.807	0.2054	4.6476	1.2874	0.1209	101.2394	520	22
Mnz1-3	0	0.2306	31.4764	1.3529	2.5855	13.3175	28.0405	2.8326	8.6204	5.0616	1.6365	0.839	0.2351	4.892	1.8284	0.0005	102.9494	487	18
Mnz1-4	0	0.2474	31.4415	1.3877	2.7358	12.969	27.3526	2.7746	8.7832	5.2915	1.72	0.9401	0.2554	4.875	2.0859	0.0187	102.8783	492	17
Mnz1-5	0	8.7736	25.9501	1.1713	1.5325	11.2827	23.6238	2.4875	7.8843	4.8592	1.483	0.4085	0.1662	5.2725	0.7834	0.0095	95.6882	476	23
Mnz1-6	0	0.4433	30.5433	1.4396	1.6401	13.1057	27.1117	2.8411	8.9877	5.454	1.7521	0.6204	0.2144	5.9661	1.0312	0	101.1506	516	21
Mnz1-7	0	0.2342	31.5159	1.1406	2.8177	13.0744	28.0741	2.8545	8.7548	4.9766	1.7313	0.9897	0.2167	4.1385	1.7506	0	102.2696	494	20
Grain 2																			
Mnz2-1	0	0.4133	30.5514	1.7532	0.8064	13.0391	28.2022	2.9738	8.6202	5.1071	1.3968	0.3926	0.2465	8.6788	0.7213	0	102.9026	504	18
Mnz2-2	0	0.3326	30.714	1.7891	1.1738	13.4121	28.4602	2.8663	8.0034	4.8343	1.3591	0.4699	0.2465	8.2169	0.8837	0.0016	102.7635	500	18
Mnz2-3	0	0.2731	30.6687	1.5503	0.8353	13.1254	28.5739	2.9114	9.059	5.4631	1.5471	0.3654	0.2203	7.1778	0.8306	0.0016	102.6029	503	20
Mnz2-4	0	0.7262	30.1109	1.8203	1.3828	13.3386	29.2157	2.9369	8.2726	4.7597	1.3655	0.5615	0.2468	6.942	0.9946	0.0627	102.7367	545	20
Mnz2-5	0	0.2305	30.5673	1.407	0.7784	12.4055	27.9958	3.0695	10.4808	6.3742	2.0298	0.3045	0.207	5.9683	0.9836	0.0189	102.821	510	21
Mnz2-6	0	0.2018	30.6737	1.4253	1.4792	13.087	27.5174	2.9386	9.118	6.0707	1.9755	0.6053	0.2138	5.7426	1.2563	0.0047	102.3098	490	20
Mnz2-7	0	0.4781	30.6493	1.6794	1.6776	13.3338	29.1117	2.8163	8.2936	5.1308	1.319	0.618	0.2121	6.7853	0.8297	0	102.9346	504	20
Mnz2-8	0	0.3964	30.748	1.8808	1.0546	13.3223	28.0702	2.8215	8.4277	4.944	1.2808	0.3484	0.2597	9.0897	0.8429	0.0032	103.4901	497	17
Grain 3																			
Mnz3-1	0	0.2392	30.9284	1.2683	2.7014	13.2478	28.0208	2.8944	8.1742	5.0345	1.6215	0.9857	0.2172	5.1351	1.4843	0.0067	101.9594	489	19
Mnz3-2	0	0.2634	30.7052	1.36	2.1965	13.4662	28.4335	2.8464	7.8834	4.8546	1.4429	0.8238	0.2242	5.8203	1.3259	0.0064	101.6526	498	19
Mnz3-3	0	0.2316	31.3339	1.3458	2.6903	13.356	28.1743	2.7739	7.8662	4.7441	1.4052	0.8581	0.2101	5.5274	1.1804	0	101.6973	504	21
Grain 4																			
Mnz4-1	0	0.254	31.329	1.3305	1.6725	13.203	27.238	2.8095	9.3507	6.2767	2.2693	0.6373	0.2011	5.1929	1.2954	0.0047	103.0646	484	20
Mnz4-2	0	0.2838	31.2619	1.4811	0.8698	13.846	28.6936	2.8684	8.7833	5.615	1.5874	0.3119	0.2153	6.5366	1.0029	0.0147	103.3717	495	20
Grain 5																			
Mnz5-1	0	0.2462	31.6826	1.2897	3.2914	13.061	26.7287	2.8062	8.8931	5.2507	1.8474	1.0444	0.2546	3.6049	2.4326	0.0125	102.4459	497	17
Mnz5-2	0	0.1978	31.6671	1.1735	1.9207	13.6039	28.3325	2.9176	8.9722	5.5162	1.933	0.7903	0.2083	3.8791	1.7395	0	102.8516	491	20
Grain6																			
Mnz6-1	0	0.4088	30.6948	1.5918	2.6632	12.6903	27.2655	2.7169	7.8363	4.8327	1.5113	0.9063	0.2591	7.2923	1.3846	0	102.0538	498	17
Mnz6-2	0	0.3988	31.0173	1.4726	4.8372	12.027	25.787	2.5293	7.4802	4.7476	1.5871	1.3216	0.3152	5.0641	2.8386	0.0025	101.4261	498	14